Friction Stir Welding of High Carbon Tool Steel (SK85) below Eutectoid Temperature †

CHUNG Young Dong*, FUJII Hidetoshi**, NAKATA Kazuhiro*** and NOGI Kiyoshi***

Abstract

The present study is concerned with applying FSW to a high carbon tool steel (0.85 wt % carbon, JIS-SK85, AISI-1080) with below and above A_1 (726° C) welding conditions and analyzing the joints as well as evaluating the joint quality. Defect-free joints can be successfully fabricated and the joint structure and the mechanical properties were investigated for both conditions. The microstructures of the above A_1 joints mainly consisted of martensite. Therefore, the micro-hardness of the above A_1 joints is significantly higher at more than 1000HV. The tensile tests results are scattered and some of the joints are fractured at the stir zone while others are fractured the base metal. On the other hand, the microstructures of the below A_1 joints consist of ferrite with globular cementite, and grain-refinement occurs because no phase transformation to the martensite structures occurs. The high carbon tool steel was successfully friction-stir was welded below the A_1 and a method has been established to obtain sound joints which show a stable fracture and a good strength.

KEY WORDS: (Hyper eutectoid steel (SK85, AISI-SAE W1-8)) (Friction Stir Welding, Butt welding) (Hardness) (A_1 point (eutectoid temperature 726ºC)) (Phase transformation) (Microstructure)

1. Introduction

The history of joining and welding of high carbon steels goes back several decades and many researchers had developed methods, techniques and materials for welding and joining of these steels. However, these are still problems: heat affected zones can easily transform to very hard and brittle martensite and weld metal does not retain its normal properties. Moreover, when welding the steel, there have been problems such as porosity, hydrogen cracking, solidification cracking, etc. Consequently, solutions are required for each problem, such as heat treatment before, during, or after welding to maintain mechanical properties[1]. **Table 1** lists the typical fusion welding problems and practical solutions for carbon and alloy steels. However, high carbon steel are still attractive materials because they have attractive properties such as high strength and good wear resistance etc.

Friction stir welding (FSW)[2] has been widely used and investigated for low melting materials such as Al, Mg and and Cu alloys[3-5]. Recently, many researchers have reported the FSW of steels and steel alloys[6-9]. In previous studies and our own studies, the steel and steel alloys were successfully welded and microstructures and mechanical properties after FSW were analyzed. It was reported that FSW achieves grain refinement in the stir zone and improved hardness and strength of the FSW joints[6-10].

However, when FSW the middle and high carbon steels with 0.45 to 1.5 percent carbon content, they can easily undergo phase transformation to the martensite structure because the peak temperature exceeds

Table 1 Typical Welding Problems and practical Solution in Carbon and Alloy steels

Typical problems	Alloy types	Solution
Porosity	Carbon and low allow steels	Add deoxidizers (Al, Ti, Mn) in filler metal
Hydrogen cracking	Steels with high carbon equivalent	Use low-hydrogen or austenitic stainless steel electrodes Preheat and post heat
Lamellar tearing	Carbon and low allow steels	Use joint designs that minimize transverse restrain Butter with a softer layer
Reheat Cracking	Corrosion and heat resisting steels	Use low heat input to avoid grain growth Minimize restraint and stress concentrations Heat rapidly through critical temperature range, if possible
Solidification cracking	Carbon and low alloy allow steels	Keep proper Mn/S ratio
Low HAZ toughness due to grain growth	Carbon and low alloy allow steels	Use carbide and nitride formers to suppress grain growth Use low heat input
Low fusion-zone toughness due to coarse columnar grains	Carbon and low alloy allow steels	Grain refining Use multipass welding to refine grains

approximately 1100 to 1200 °C. Sato et al.[12] discussed very high carbon steel which had a 1.02 wt% carbon content that underwent a microstructural evolution during FSW. However, the joint had a martensitic structure in the welded joint. Therefore, they required heat treatment before, during, or after welding to maintain their mechanical properties. In our previous study,[13] high carbon steel, which had a 0.7 wt% carbon content, was successfully welded and showed no transformation to the martensite structure in the joint although martensite was observed at the top of the stir zone.

Although the FSW has attracted attention as a useful joining process that provides superior characteristics when compared to conventional fusion welding, the welding of higher carbon steels is more difficult than that of the lower carbon steels because of the greater tendency of martensite formation when the peak temperature exceeds the A_1 (eutectoid temperature 726ºC). In this case, the joint requires heat treatment before, during, or after welding to maintain its mechanical properties.

In the present study, the butt-welding of high carbon tool steel (SK85, AISI 1080), which is a 0.85 wt% high carbon steel, was inspected below and above the A_1 welding conditions along with evaluation of the joint quality using a load controlled FSW machine.

2. Experimental

The base material was a high carbon tool steel with 0.85 wt % carbon content. The chemical composition of this steel is listed in **Table 2**. The initial microstructure of the SK85 steel is a ferrite matrix with globular cementite (see **Fig. 1**). Butt welding is conducted on the rectangular plates with the dimensions of 1.6mm thick, 250mm long and 50mm wide. The welding experiments were performed using a load-controlled FSW machine and the welding tool was made of a WC-based material and the tool was tilted 3° from the plate normal direction.

The rotation speeds were from 100 to 400rpm and the welding speeds were 100 and 800mm/min as shown in **Table 3**. Ar shielding gas was used during the FSW. For the purpose of below A_1 welding and the evaluation of the below A_1 joint quality, a minimum heat input was used for the materials. The welding of the above A_1 used the typical condition when the steel was welded by FSW.

Table 2 Chemical compositions of SK85 steel.

Type	Chemical composition in mass %								
	C	Mn	Si	Cr	P	Cu	Ni	S	Al
SK85	0.85	0.42	0.19	0.147	0.017	0.01	0.01	0.003	0.001

Table 3 Welding parameters.

Welding parameters		
Rotation speed (rpm)	Welding speed (mm/min)	Revolution pitch (mm/rev)
100–400	100–800	0.5–2
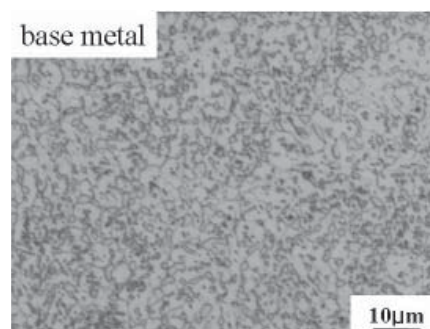
Fig.1 Microstructure of high carbon tool steel (SK85)

Fig.2 Schematic drawing showing the location of micro-hardness measurements

Optical microscopy (OM) and SEM observations of the microstructure of each FSW joint and fracture surface were carried out. The specimen for the optical microscopy observations was cut perpendicular to the welding direction and etched using a 5 vol.% nitric acid + 95 vol.% ethanol solution. The tensile tests for the joints and the stir zone were performed using three tensile specimens cut perpendicular to the welding direction. The Vickers hardness test profile of the welded joint was measured on the cross section perpendicular to the welding direction and included the upper, center and bottom, as shown in **Fig. 2**, with a 0.98 N load for 15s; the upper and bottom had a 0.1mm gap and measured at an interval of 0.5mm.

3. Results

3-1. Microstructure of joints

Fig. 3(a)-(c) shows cross sections of the welded joints for the above A_1 condition which were welded at different welding speeds with a constant rotation speed of 400rpm. Although all the conditions successfully produced defect free joints, the joints structure from the top to the bottom were different, and were divided into the below and above A_1 regions, except for at 200mm/min welding speed, because the peak temperature decreased with the increasing welding speed. Therefore, in this study, the 400 rpm rotation speed and 200mm/min welding speed were used to compare the below A_1 conditions. For all the joints at the 400rpm rotation speeds, two regions are observed in the SZ, as shown in **Fig. 3(a)**. The black part, corresponding to the martensite-pearlite structure, was heated above A_1 and the white part, corresponding to the fine ferrite -globular cementite structure, was not heated above A_1. The below
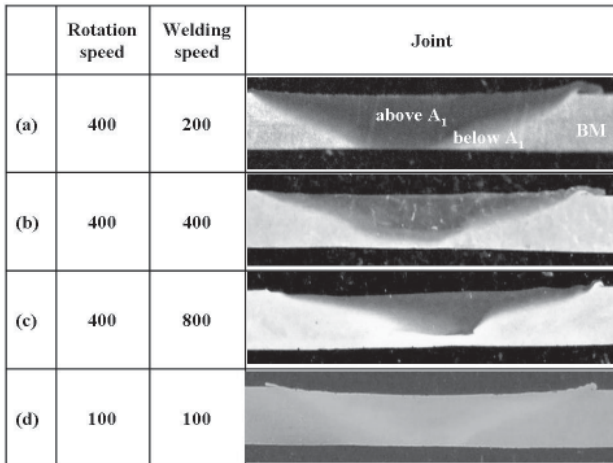
Fig.3 Cross sections of the below and above A_1 joints

A_1 condition was achieved under the conditions of 100rpm rotation speed and 100mm/min welding speed, in which a sound defect-free joint with full penetration was obtained as shown in **Fig. 3(d)**.

Fig. 4 shows the microstructures of the stir zone: **(a, d)** upper part, **(b, e)** center part and **(c, f)** bottom part shows the microstructures of the joint. For the 100rpm rotation speed and 100mm/min welding speed conditions **Fig. 4(a, b, c)** the entire structure of the joint became fine ferrite with globular cementite which is the same composition microstructure as that in the base metal. Thus, the 100rpm rotation speed and 100mm/min welding speed condition should be successfully done below A_1, since no transformation occurs and no martensite forms. Additionally, the ferrite-grain refinement occurring is due to dynamic recrystallizaion. **Fig. 4(d, e, f)** shows the microstructures of the stir zone under the welding condition of a 400 rpm rotation speed and 200mm/min welding speed.
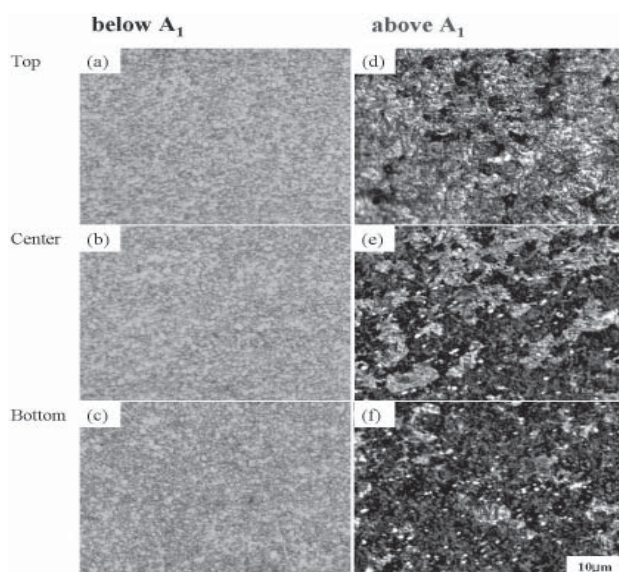

Fig.4 Microstructures of the below and above A_1 joint

All of the joint structures consisted of a mixture of martensite and pearlite. The martensite fraction decreased with depth from top (approximately 65%) to bottom (near 28%). It is related to a decrease in the peak temperature from top to bottom during welding. Although the distribution and quantity of the martensite increases near the surface, each part of the stir zone had a martensitic structure. Thus, the peak temperature should exceed A_1 from the upper to bottom and then the martensite joint structure is easily formed.

### 3-2. Mechanical properties of joints

The hardness profile of the below A_1 joint, which was made at a 100 rpm rotation speed and 100 mm/min welding speed, is shown in **Fig. 5(a)**. The hardness result of the below A_1 joint corresponded to the microstructures result; all of the joint structure became fine ferrite + globular cementite, and no transformation occurred and no martensite was formed. Thus, the maximum hardness is slightly greater than the base metal. This two-phase structure is the optimal structure which produces a high toughness and ductility[13]. The hardness profile of the above A_1 FSW joint, which had a 400 rpm rotation speed and 200 mm/min welding speed condition, is shown in **Fig. 5(b)**.

The hardness of the base metal is approximately 220 HV; whereas the maximum hardness of the upper and center regions of the welded joints is greater than 1000 HV which is still higher than the typical hardness data of the high carbon steel martensite (around 900Hv)[14]. Generally, recrystallization occurs in the stir zone which has a finer grain structure than the base metal. Furthermore, the microstructure consists of two types of martensite and perlite and these conditions of the mixture provide the plastic interaction such as precipitation hardening. Thus, the maximum hardness of the stir zone is greater than the typical hardness of the high carbon steel martensite. The maximum hardness of the joints decreases with the position reaching the bottom surface. The reason for the different micro-hardnesses in the upper, center and bottom parts is their different peak temperatures and is related to the different distribution and quantity of the martensite. Based on these hardness results, the peak temperature exceeded A_1 and the joint structure easily formed the martensite.

The following tensile and elongation results are shown in **Figure 6**. The tensile strength and elongation are denoted by the open circles, and the bars show the average value of the data. The strength of the below A_1 joints slightly increased when compared to the base metal because all of the joint structures became a fine ferrite with globular cementite, and grain refinement then occurred. Therefore, the below A_1 joints show the stable elongation. Regarding the strength of the above A_1 joints, the tensile test results are scattered because they are dependent on the distribution and quantity of the martensite.
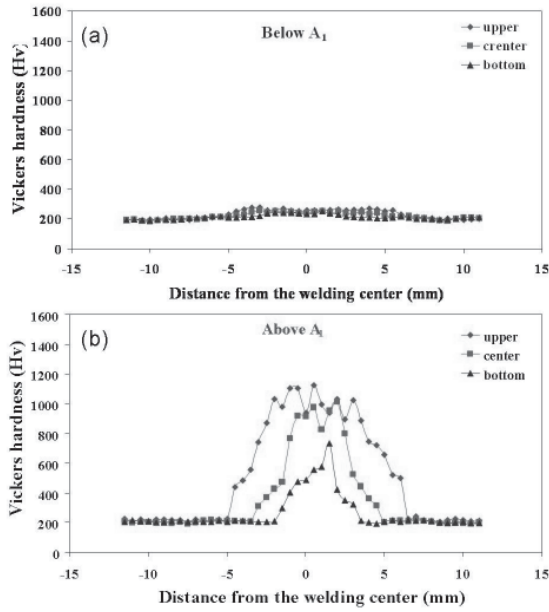
Fig.5 Horizontal micro-Vickers hardness profiles under the below(a) and above(b) A_1 conditions
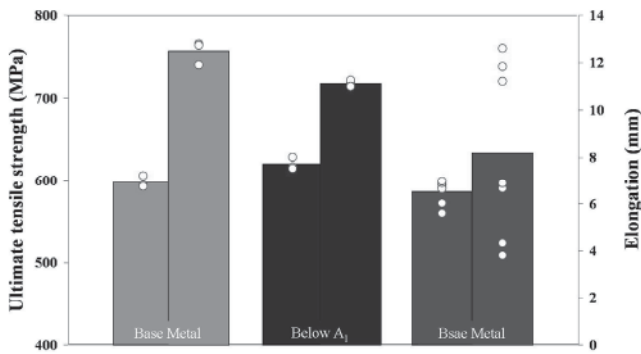

Fig.6 Tensile strength and elongation of FSW joint for SK85

When compared to the tensile strength value of each joint condition, it is difficult to find a significant reason for the similar tensile strength value.

However, the microstructures of the samples are completely different from each other. This means that the strengthening mechanisms are different from each other. Additionally, the uniform elongation data are completely different from each other, in which the base metal and below A_1 joints show a stable elongation but the above A_1 joints show an unstable elongation, so that it appears difficult to find the physical reason for the similar strength value.

Figure 7 shows the appearance of the joints after the tensile test; joints of the below A_1 are fractured at the base metal., however, some of joints of the above A_1 are fractured at the joints, while the others at the base metal. These results indicated that the below A_1 joint is a stronger and more stable joint that the above A_1 joint.
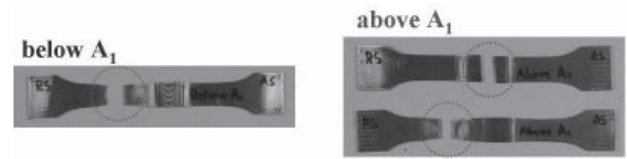
Fig.7 Appearance of joints after tensile test
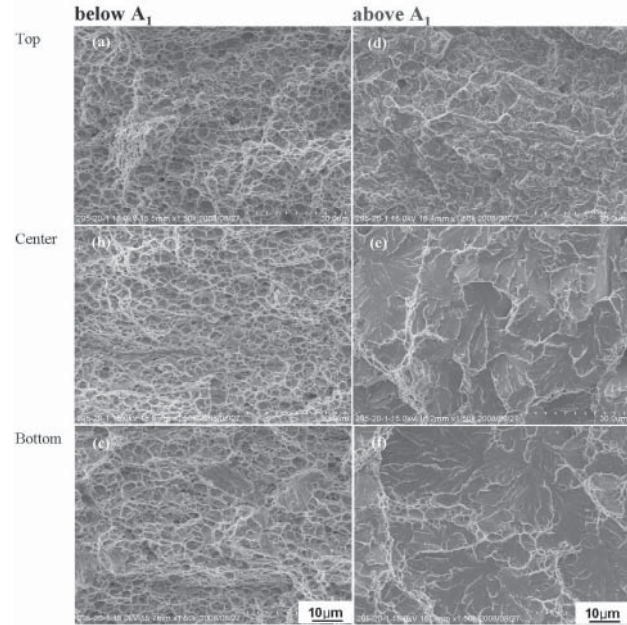
Fig.8 SEM images of fracture surface for the stir zone specimens

The small size specimens whose gage area includes only the stir zone were examined in order to evaluate the mechanical properties of the stir zone itself. The tensile strength of the SZ of the below A_1 specimen is approximately 830MPa which is much greater than that of the base metal. Accordingly, all the below A_1 joints were fractured at the base metal for the normal tensile test.

Figure 8 shows SEM images of the fracture surfaces of the stir zone specimens. **Fig. 8(a, b, c)** and **(d, e, f)** are the fracture surface of the below and above A_1 joints, respectively. On the fracture surface of the below A_1 stir zone exhibited only a dimple pattern **(a, b)**, although the bottom of the stir zone **(c)** has a mixed mode of fracture in which the fracture surface almost appeared as a dimple pattern. This results indicates that the microstructure of the fine ferrite matrix with globular cementite generated by the below A_1 welding is ductile and useful for improvement of the joint of the hyper eutectoid steel. However, the fracture surface of the above A_1 stir zone, the fracture surface mainly appeared as a river pattern **(d, e)** which was related to the brittle fracture and a few parts showed a dimple pattern **(f)** which was related to the ductile fracture. It was associated with the scattering of the high carbon martensite structure in the above A_1 joint.

4. Conclusions.

In summary, high carbon tool steel was successfully friction-stir welded. When the welding was performed below A_1, no transformation occurred and no martensite formed, and the below A_1 joint was successfully friction-stir welded at a 100rpm rotation speed and 100 mm/min welding speed. The tensile results of the above A_1 joints were scattered because they are dependent on the distribution and quantity of the martensite. The fracture behavior and fracture surface of the stir zone were affected by the welding conditions. The above A_1 joint appeared as a river pattern and the below A_1 joint showed a dimple pattern. Comparing the below A_1 and above A_1, the mechanical properties of the below A_1 joint include a good toughness and ductility, because the joint had a fine ferrite-globular cementite structure, and grain-refinement occurred.

References

1) S. Kou: 'Welding Metallurgy', 2nd edn, 393-426, 2003
2) W. M. Thomas, P. L. Threadgill and E. D. Nicholas: *Sci. Technol.Weld. Joining*, 1999, 4, 365.
3) C.J. Dawes, W.M. Thomas, Weld. J, 75, 41, (1996).
4) J.I.Skar1, H. Gjestland, L.D. Osterkamp, D.L.Albright, Magnesium Technology (2004).
5) H. S. Park, T. Kimura, T. Murakami, Y. Nagano, K. Nakata and M.Ushio, *Mater. Sci. Eng. A*, A371, 160, (2004).
6) A. P. Reynolds, W. Tang, T. Gnaupel-Herold and H. Prask: *Scr.Mater.* , 2003, 48, 1289.
7) H. Fujii, R. Ueji, Y. Takada, H. Kitahara, N. Tsuji, K. Nakata and K.Nogi: *Mater. Sci. Eng. A.*, (2006),423, 324-330.
8) H. Fujii, L. Cui, N. Tsuji, M. Maeda, K. Nakata and K. Nogi: *Mater.Sci. Eng. A*, 2006, A429, 50.
9) C. D. Sorensen, T. W. Nelson and S. M. Packer: Proc. of 3rd Int. Symp. Friction stir welding, TWI, Cambridge, UK, 2001, CDROM.
10) Miles, M.P., Pew, J., Nelson, T.W., Li, M: Sci. Technol. Weld. Join., 2006, 11, 384-388
11) A. P. Reynolds, W. Tang, T. Gnaupel-Herold and H. Prask: *Scr.Mater.*, 2003, 48, 1289.
12) Y.S. Sato, H. Yamanoi, H. Kokawa, T. Furuhara, Scripta materialia, 2007, 57, 557-560
13) L. Cui, H. Fujii, N.Tsuji, K. Nogi: Scripta materialia 56 (2007) 637-640
14) G. Krauss: 'STEELS: Heat Treatment and Processing Principles', 1990 edn, 145, 1989